

Supporting Information

Engineering High-Energy, High-Rate NASICON Cathodes via Cu Doping and Microwave-Induced Grain Refinement for Sodium-Ion Batteries

Zhao XIE[†], Jun WU[†], Yali SUN, Qiumei WAN, Wenwen CUI, Qingqing GE, Dai LU, Chunyang LI*,
Hong LUO*

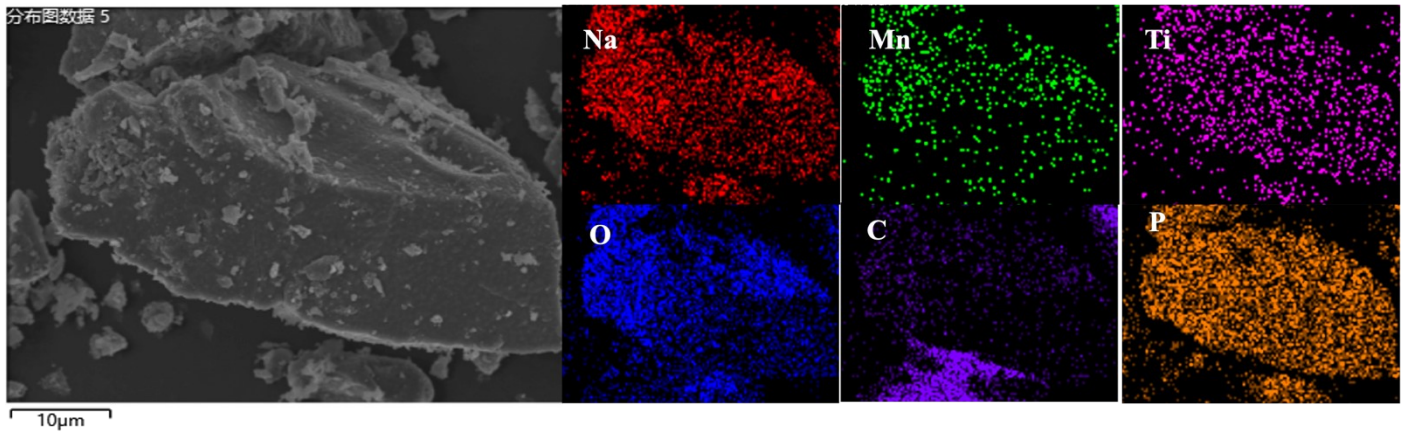


Figure S1. EDS mapping images and SEM images of NMTP treated by microwave heating way

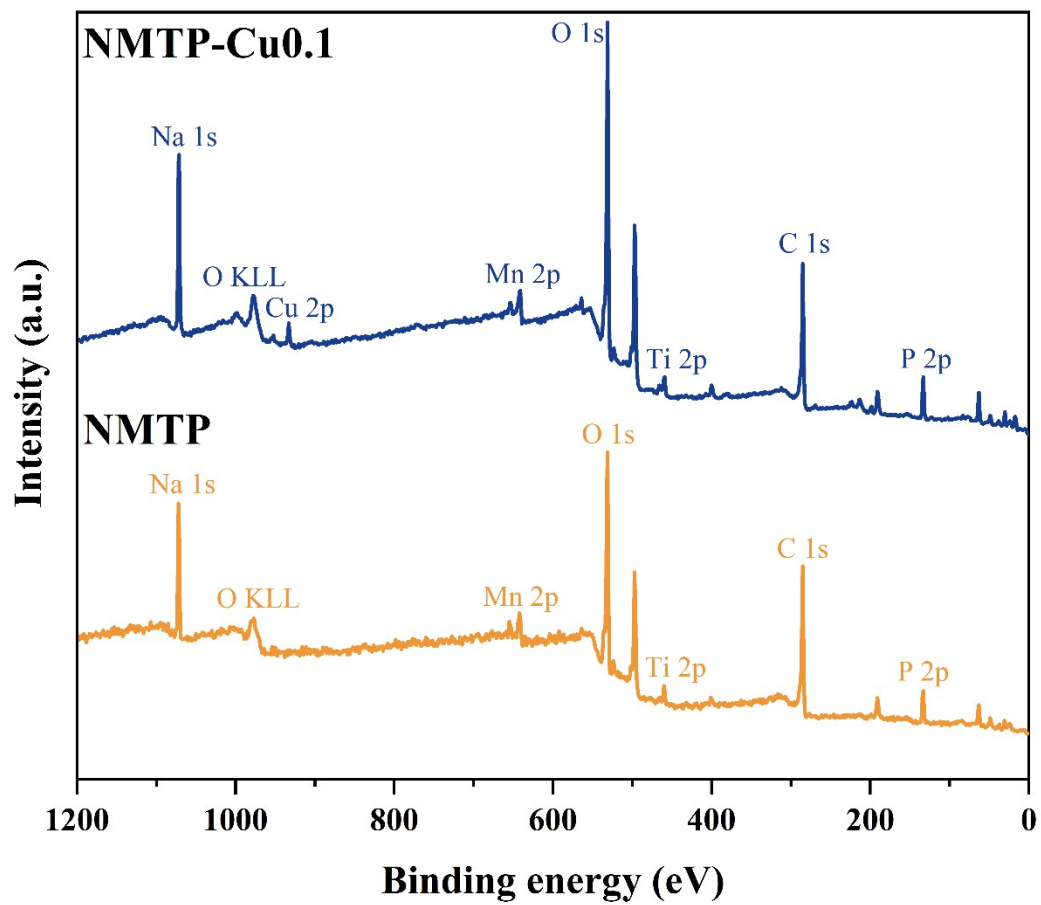


Figure S2. The XPS survey spectra of the NMTP and NMTP-Cu_{0.1}.

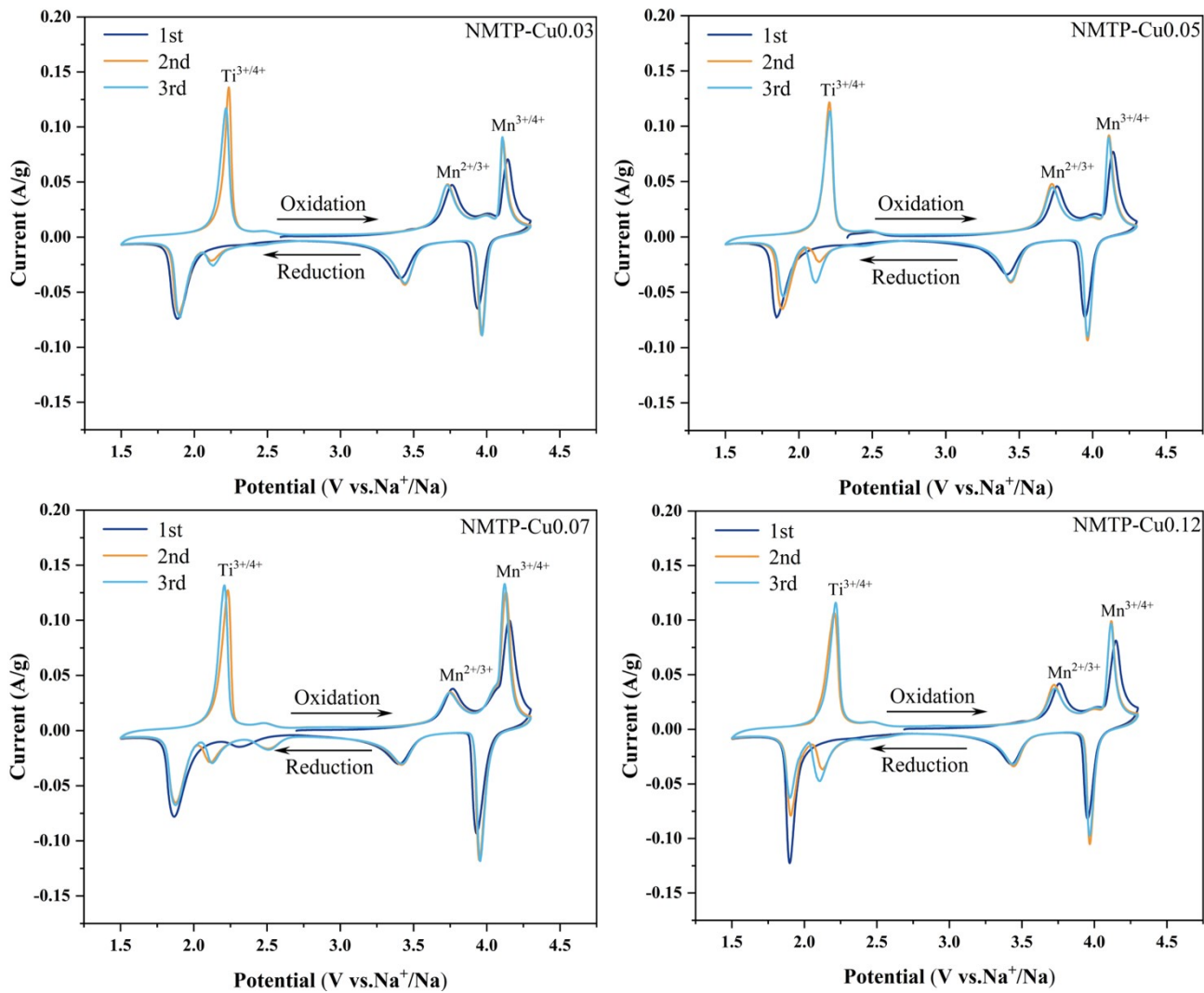


Figure S3. CV curves of NMTP-Cu_x (x=0.03, 0.05, 0.07, 0.12) series.

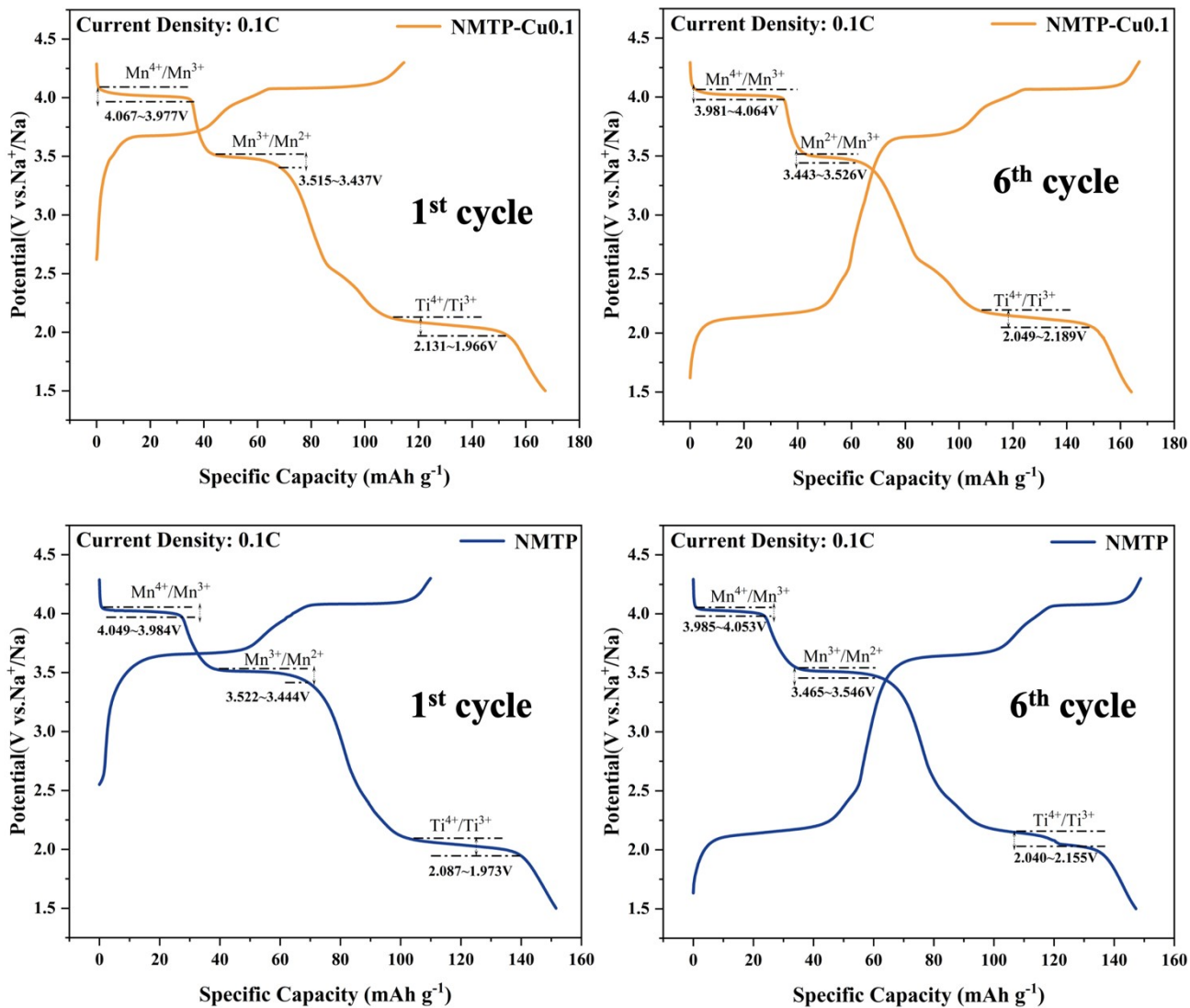


Figure S4. GCD profiles of NMTP-Cu_{0.1} and NMTP at first cycle and sixth cycle.

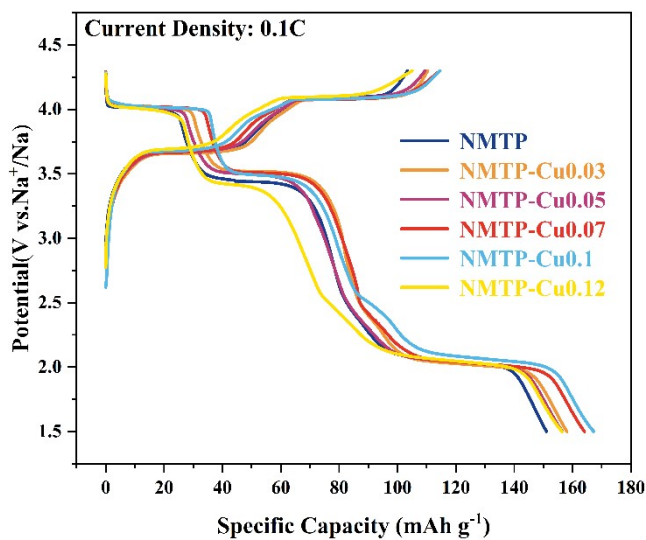


Figure S5. GCD curves and of NMTP-Cu_x (x=0, 0.03, 0.05, 0.07, 0.1, 0.12) series at 0.1C.

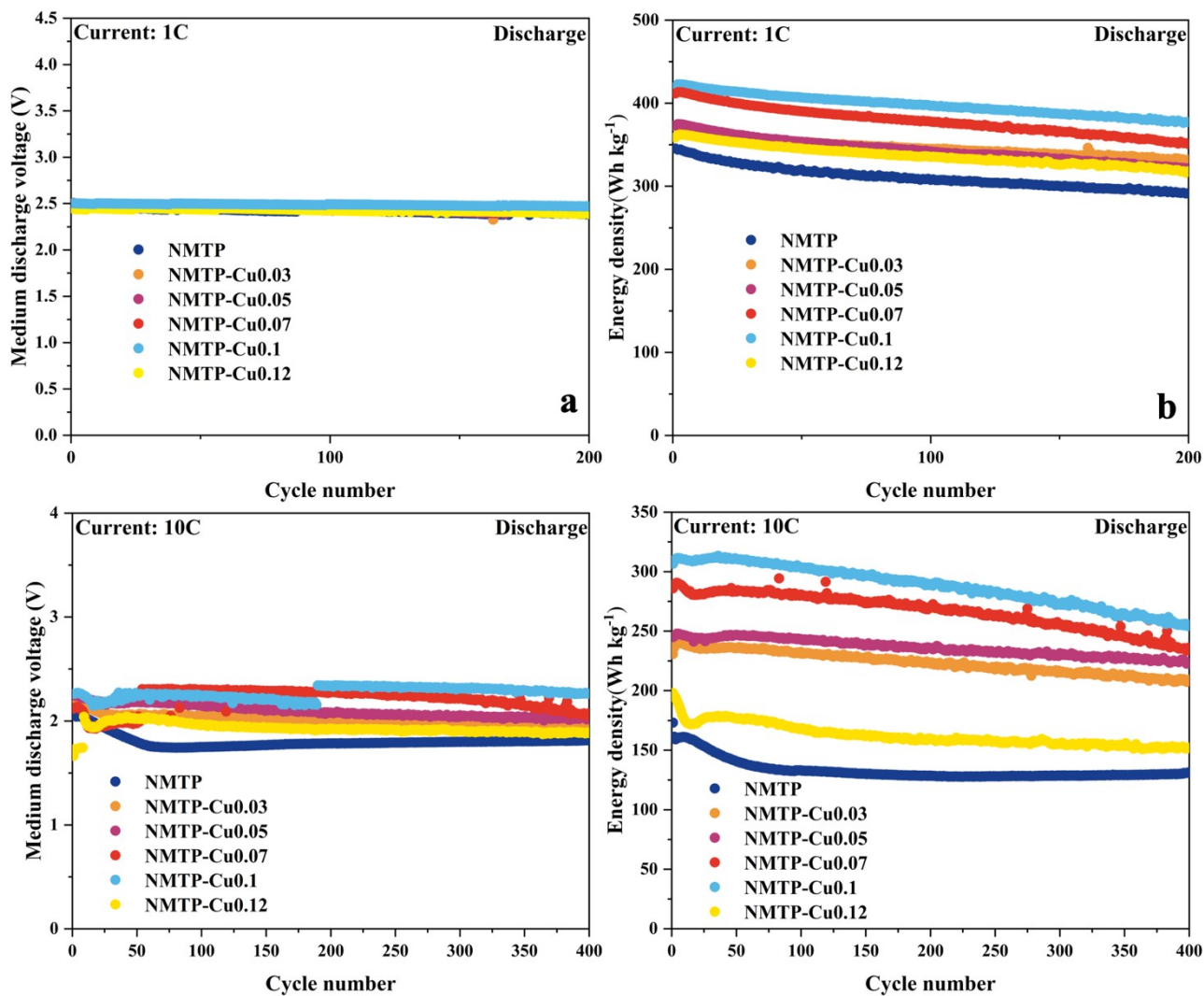


Figure S6. Medium voltage and energy density of NMTP-Cu_x (x=0.03, 0.05, 0.07, 0.12) series.

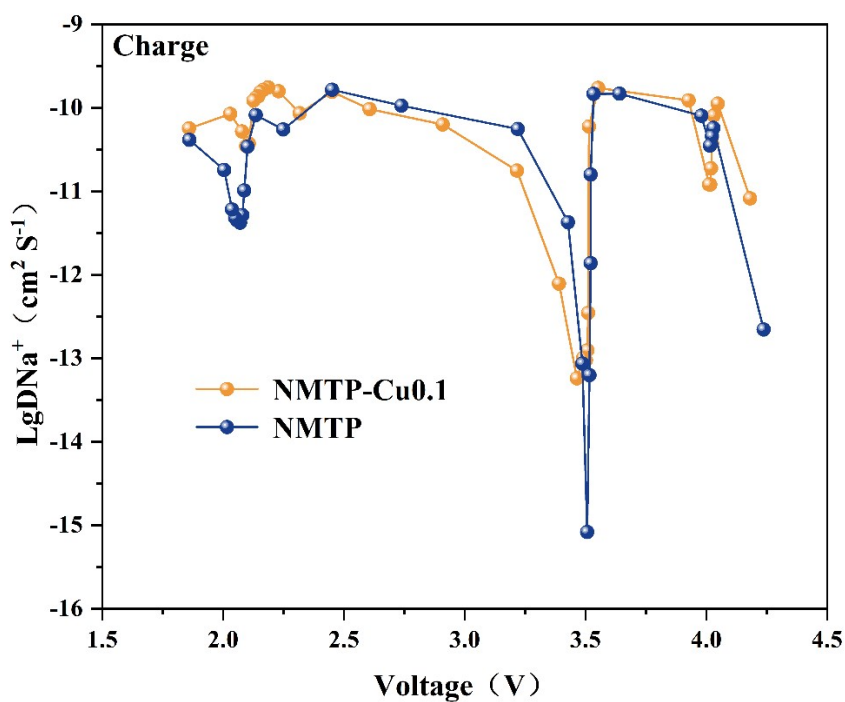


Figure S7. Plots of the $\log \left(\text{Na}^+ \right)$ versus cell potential profiles for NMTP-Cu_{0.1} and NMTP during charge process at 0.1C.

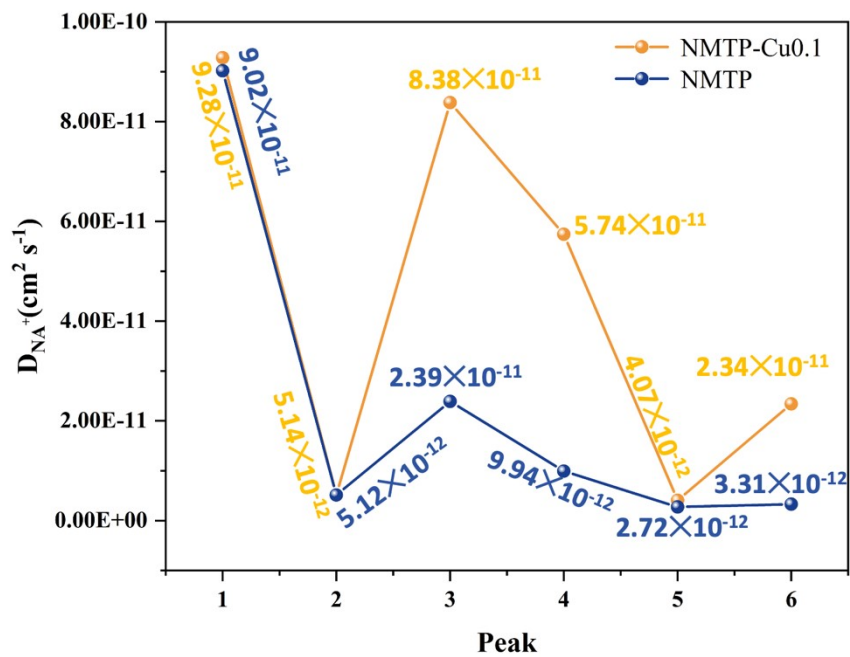


Figure S8. Calculation of Na⁺ diffusion coefficients by CV.

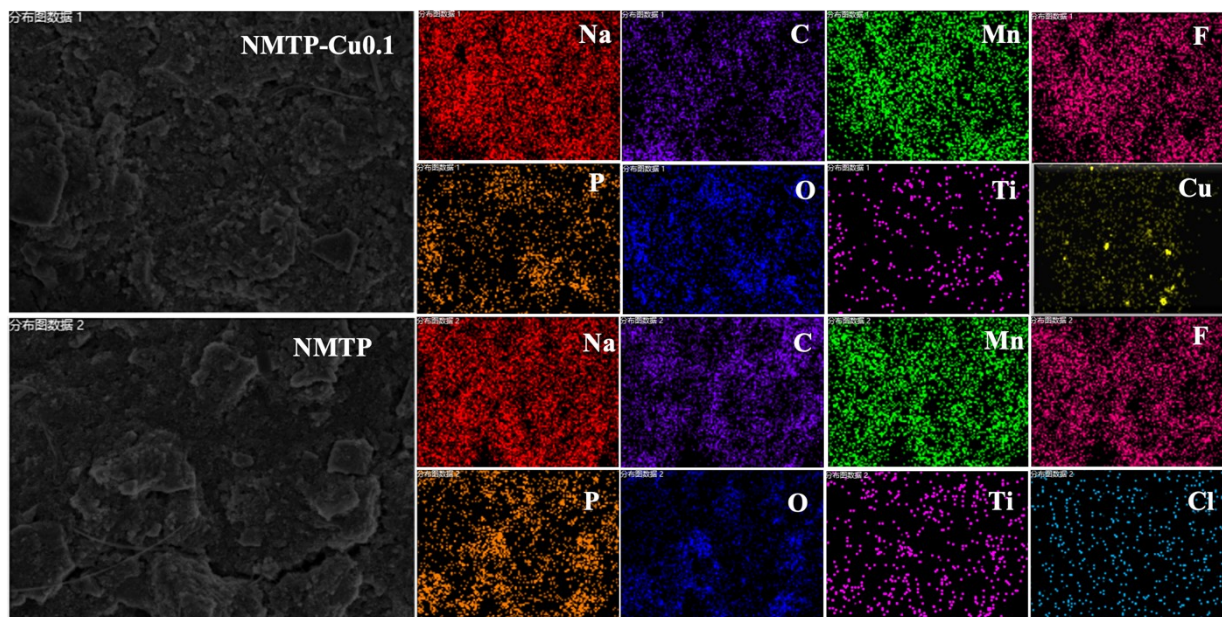


Figure S9. EDS mapping images and SEM images of NMTP-Cu_{0.1} and NMTP after 3000 cycles.

Table S1. Stoichiometry of compounds determined by ICP-OES.

Copper ion doping content	Measured atomic ratio/wt%					Chemical formula
	Na	Mn	Cu	Ti	P	
0	2.097	1.070	/	1.011	2.650	Na _{2.10} Mn _{1.07} Ti _{1.01} (PO ₄) ₃
0.03	2.635	0.996	0.030	1.014	2.541	Na _{2.64} Mn _{0.99} Cu _{0.03} Ti _{1.01} (PO ₄) ₃
0.05	2.643	0.992	0.050	1.017	2.593	Na _{2.65} Mn _{0.99} Cu _{0.05} Ti _{1.01} (PO ₄) ₃
0.07	2.673	0.960	0.070	1.019	2.520	Na _{2.68} Mn _{0.96} Cu _{0.07} Ti _{1.01} (PO ₄) ₃
0.10	2.733	0.940	0.090	1.019	2.543	Na _{2.74} Mn _{0.94} Cu _{0.10} Ti _{1.01} (PO ₄) ₃
0.12	2.679	0.917	0.120	1.012	2.567	Na _{2.68} Mn _{0.92} Cu _{0.12} Ti _{1.01} (PO ₄) ₃

Table S2. The structure information details of NMTP derived from Rietveld Refinement.

Space group = R-3c			Rp = 5.02%		Rwp = 6.37%	
a (Å) = b (Å) = 8.84123			c(Å) = 21.62726		$\alpha(^{\circ}) = 90$	
$\beta(^{\circ}) = 90$			$\gamma(^{\circ}) = 120$		V (Å ³) = 1464.056	
Atom	X	Y	Z	Wyckoff site	Occupancy	Uiso
Na1	0.00000	0.00000	0.00000	6b	0.705	0.02225
Na2	0.64224	0.00000	0.25000	18e	0.767	0.01372
Mn	0.00000	0.00000	0.14918	12c	0.492	0.00535
Ti	0.00000	0.00000	0.14918	12c	0.508	0.00535
P	0.29838	0.00000	0.25000	18e	1.000	0.00679
O1	0.01360	0.20900	0.19320	36f	1.000	0.00283
O2	0.18630	0.17210	0.08520	36f	1.000	0.00450

Table S3. The structure information details of NMTP-Cu_{0.1} derived from Rietveld Refinement.

Space group = R-3c			Rp = 5.81%		Rwp = 7.31%	
a (Å) = b (Å) = 8.83327			c(Å) = 21.61683		$\alpha(^{\circ}) = 90$	
$\beta(^{\circ}) = 90$			$\gamma(^{\circ}) = 120$		V (Å ³) = 1460.715	
Atom	X	Y	Z	Wyckoff site	Occupancy	Uiso
Na1	0.00000	0.00000	0.00000	6b	0.664	0.02200
Na2	0.64250	0.00000	0.25000	18e	0.720	0.01399
Mn	0.00000	0.00000	0.14920	12c	0.457	0.00568
Ti	0.00000	0.00000	0.14920	12c	0.495	0.00568
Cu	0.00000	0.00000	0.14920	12c	0.048	0.00568
P	0.29838	0.00000	0.25000	18e	1.000	0.00728

O1	0.01360	0.20900	0.19320	36f	1.000	0.00311
O2	0.18630	0.17210	0.08520	36f	1.000	0.00489

Table S4. Comparison between NMTP-Cu_{0.1} and other reported NMTP cathodes for SIBs.

Materials	Low-rate capacity	High-rate capacity	Capacity stability
NMTP/C ₋₆₅₀ ^[1]	160mAh/g at 0.2C	129mAh/g at 2C	92% after 500 cycles at 2C
10%Cr-NMTP ^[2]	126.72mAh/g at 0.1C	85.99mAh/g at 5C	73.74% after 500cycles at 10C
NMTP-V ₃ ^[3]	133.6mAh/g at 0.1C	69.1mAh/g at 10C	73.6% after 500cycles at 1C
Na ₃ MnTi(PO ₄) ₃ -CNF ^[4]	124.38mAh/g at 0.05C	77.6mAh/g at 20C	59.6% after 1000 cycles at 1C
Na ₃ MnTi(PO ₄) ₃ WC ^[5]	123.0mAh/g at 0.1C	73.0mAh/g at 2C	92% after 1000 cycles at 2C
Na _{3.5} MnTi _{0.93} Co _{0.07} (PO ₄) ₃ ^[6]	150.5mAh/g at 0.1C	112.0mAh/g at 10C	94.7% after 100 cycles at 1C
Na _{3.4} Mn _{1.2} Ti _{0.8} (PO ₄) ₃ ^[7]	141.9mAh/g at 0.1C	96.59mAh/g at 2C	97.1% after 500 cycles at 2C
NMTP-Fe _{0.02} ^[8]	153.2mAh/g at 0.1C	139.5mAh/g at 5C	81.5% after 800 cycles at 5C
This Work	167.25mAh/g at 0.1C	120.85mAh/g at 10C	86.7% after 400 cycles at 10C

Table S5. Discharge specific capacity of NMTP-Cu_x (x=0, 0.03, 0.05, 0.07, 0.1, 0.12) series at different rates.

Samples (mAh/g)	0.1C	0.2C	0.5C	1C	2C	5C	10C	0.1C
NMTP	151.60	139.13	129.40	122.37	114.52	100.74	82.60	139.82
NMTP-Cu0.03	158.06	147.17	138.65	131.81	124.04	110.22	93.53	148.66
NMTP-Cu0.05	160.52	145.76	136.32	129.16	121.22	107.05	88.53	148.29
NMTP-Cu0.07	164.11	151.30	142.06	135.77	128.55	115.07	95.19	153.74
NMTP-Cu0.1	167.25	158.12	150.36	144.83	139.12	126.87	101.36	159.63
NMTP-Cu0.12	156.44	143.31	133.71	126.03	118.07	102.87	71.52	145.74

Table S6. Discharge energy density of NMTP-Cu_x (x=0, 0.03, 0.05, 0.07, 0.1, 0.12) series at ranging current density.

Samples (Wh/kg)	Energy density at 0.1C	Energy density at 1C	Energy density at 10C
NMTP	443.44	345.49	173.14
NMTP-Cu0.03	459.56	372.49	230.75
NMTP-Cu0.05	456.23	373.31	245.01
NMTP-Cu0.07	474.19	411.69	285.89
NMTP-Cu0.1	481.89	419.51	306.57
NMTP-Cu0.12	432.74	358.85	198.01

Table S7. Discharge specific capacity of N NMTP-Cu_x (x=0, 0.03, 0.05, 0.07, 0.1, 0.12) series at 1C after 200 cycles.

Samples	First cycle discharge specific capacity/(mAh/g)	Capacity retention(%)	columbic efficiency (%)
NMTP	127.26	88.78	99.68
NMTP-Cu0.03	136.98	91.25	99.21
NMTP-Cu0.05	137.34	89.08	99.69
NMTP-Cu0.07	149.56	88.32	99.67
NMTP-Cu0.1	152.39	91.54	99.66
NMTP-Cu0.12	134.28	90.17	99.64

Table S8. Discharge specific capacity of NMTP-Cu_x (x=0, 0.03, 0.05, 0.07, 0.1, 0.12) series at 10C after 400 cycle.

Samples	First cycle discharge specific capacity (mAh/g)	Capacity retention(%)	columbic efficiency (%)
NMTP	76.97	82.98	99.89
NMTP-Cu0.03	97.55	93.43	99.89
NMTP-Cu0.05	100.11	95.04	99.88
NMTP-Cu0.07	116.15	86.20	99.78
NMTP-Cu0.1	120.85	86.74	99.84
NMTP-Cu0.12	89.64	79.77	99.88

Table S9. Dynamic parameters of NMTP-Cu_x (x=0, 0.03, 0.05, 0.07, 0.1, 0.12) series obtained via equivalent circuit fitting.

Samples	R _s (Ω)	R _f (Ω)	R _{ct} (Ω)	σ(Ω cm ² s ^{-1/2})	D _{Na+} (cm ² s ⁻¹)
NMTP	4.809	16.350	230.700	151.900	2.998×10 ⁻¹³
NMTP-Cu0.03	5.114	10.860	115.600	107.300	4.004×10 ⁻¹³
NMTP-Cu0.05	5.773	11.290	128.100	112.000	3.675×10 ⁻¹³
NMTP-Cu0.07	4.919	10.170	99.970	105.800	4.118×10 ⁻¹³
NMTP-Cu0.1	5.045	8.585	95.610	73.700	8.487×10 ⁻¹³
NMTP-Cu0.12	4.646	7.353	153.000	71.900	7.917×10 ⁻¹³

Table S10. Comparison of Na⁺ diffusion coefficients derived from GITT, CV and EIS methods.

Method	NMTP	NMTP-Cu _{0.1}	Trend	Notes
GITT	6.41×10 ⁻¹¹ (average)	7.54×10 ⁻¹¹ (average)	↑	Apparent diffusivity; Including phase boundary contribution
CV	10 ⁻¹¹ ~ 10 ⁻¹² (range)	10 ⁻¹¹ ~ 10 ⁻¹² (range)	↑	Pear-dependent; Consistent with GITT order magnitude

References

- [1] T. Zhu, P. Hu, X. Wang, Z. Liu, W. Luo, K. A. Owusu, W. Cao, C. Shi, J. Li, L. Zhou, L. Mai. Realizing three-electron redox reactions in NASICON-structured $\text{Na}_3\text{MnTi}(\text{PO}_4)_3$ for sodium-ion batteries. 2019, 9, 1803436
- [2] Y. Jiang, Y. Wang, X. Li, J. Zhang, K. Chen, J. Liang, L. Zhao, C. Dai. a Chromium doped NASICON-structured $\text{Na}_3\text{MnTi}(\text{PO}_4)_3/\text{C}$ cathode for high-performance sodium-ion batteries. *Colloids and Surfaces A: Physicochemical and Engineering Aspects*. 2022, 649, 129340.
- [3] Y. Jiang, J.n Liang, K. Song, K. Chen, X. Li, L. Zhao, C. Dai, J. Zhang, Y. Wang. Benefits of vanadium doping in $\text{Na}_3\text{MnTi}(\text{PO}_4)_3/\text{C}$ as a potential candidate for sodium-ion batteries. *Materials Chemistry and Physics*. 2022, 282, 125938.
- [4] D. M. Conti, C. Urru, G. Bruni, P. Galinetto, B. Albini, V. Berbenni, A. Girella, D. Capsoni. $\text{Na}_3\text{MnTi}(\text{PO}_4)_3/\text{C}$ Nanofiber Free-Standing Electrode for Long-Cycling-Life Sodium-Ion Batteries. *Nanomaterials*. 2024, 14, 804.
- [5] F. Xia, M. Ahangari, J. Wu, D. H. Tran, X. Zhou, Z. Chen, H. Luo, M. Zhou. Reductive Carbon as an Additive Enables the High Capacity and Durability of NASICON Structured Sodium-Ion Batteries. 2025, 8, 4355.
- [6] N. Chen, X. Qin, Z. Guo, A. Li, Y. Zhang, T. Yang, A. Feng, Y. Qin. Co doping in NASICON-structured $\text{Na}_{3.5}\text{MnTi}(\text{PO}_4)_3$ enables superior structural stabilization and rate performance. *Journal of Alloys and Compounds*. 2024, 1005, 176130.
- [7] C. Li, S. Pu, J. Liu, Y. Huang, J. Chen, X. Xiang, L. Fu, C. Zou, X. Li, M. Wang, Y. Lin, H. Cao. Enhancing Kinetics in Sodium Super Ion Conductor $\text{Na}_3\text{MnTi}(\text{PO}_4)_3$ through Microbe-Assisted and Structural Optimization. 2024, 16, 17, 22035.
- [8] M. Yang, S. Deng, S. Cheng, J. Zhao, S. Li, Y. Bai. Unlocking fast and reversible sodium intercalation in $\text{Na}_3\text{MnTi}(\text{PO}_4)_3$ cathode toward high performance sodium-ion batteries. *Nano Research*. 2025, 18, 94907561.